MOLECULAR IMAGING AND BIOLOGY

Mol Imaging Biol (2019) 21:558–566
DOI: 10.1007/s11307-018-1263-2

Published Online: 13 August 2018

RESEARCH ARTICLE

# Combined Early and Late [$^{68}$Ga]PSMA-HBED-CC PET Scans Improve Lesion Detectability in Biochemical Recurrence of Prostate Cancer with Low PSA Levels

M. Hohberg,[1,2] C. Kobe,[1,2] P. Täger,[1,2] J. Hammes,[1,2] M. Schmidt,[1,2] F. Dietlein,[1,3] M. Wild,[1] A. Heidenreich,[2,4] A. Drzezga,[1,2] M. Dietlein[1,2]

[1]*Department of Nuclear Medicine, University Hospital of Cologne, Kerpener Str. 62, 50937, Cologne, Germany*
[2]*Cancer Center Cologne, University Hospital of Cologne, Cologne, Germany*
[3]*Department of Medical Oncology, Dana-Farber Cancer Institute, Boston, MA, 02215, USA*
[4]*Department of Urology, University Hospital of Cologne, Cologne, Germany*

**Abstract**

*Purpose:* Our aim was to evaluate the benefit of early (1 h post-injection (p.i.)) and late (3 h p.i.) [$^{68}$Ga]PSMA-HBED-CC positron emission tomography (PET)/x-ray computed tomography (CT) imaging for detection of biochemical recurrence (BCR) of prostate cancer (PCa).

*Procedures:* Seventy patients with BCR of the PCa and prostate-specific antigen (PSA) levels of less than 2.0 μg/l were subjected to [$^{68}$Ga]PSMA-HBED-CC PET (mean injected activity 180 MBq). While early imaging contained whole body scans, late imaging was confined to the pelvis and the lower abdomen. Uptake in suspicious lesions was analyzed by peak and maximum standardized uptake values ($SUV_{peak/max}$). Tumor-to-background ratios were calculated for all lesions in which the liver served as reference organ. The Wilcoxon matched-pair signed-rank test was used to compare the uptake in suspicious lesions between early and late imaging. Follow-up data were used to validate the existence of the additionally detected lesions.

*Results:* Forty-four of the 70 patients thus examined were interpreted as PSMA-positive in early and/or late scans while 26 remained without suspicion of PSMA tracer uptake. A total of 70 suspicious lesions were analyzed. Ten tumor-suspicious lesions from seven different patients were better or exclusively visible in the late measurements while three tumor-suspicious lesions from three different patients were better or exclusively visible in the early images. A validation by follow-up data was possible for 11 of these 13 additionally detected lesions. In direct comparison between early and late imaging, the mean $SUV_{max}$ in PSMA-positive lesions was 74 % higher ($p < 0.001$) and the mean $SUV_{peak}$ was 36 % higher ($p = 0.001$) in the late scans. The $SUV_{mean}$ in the reference regions was decreasing in the late measurements, whereas the mean TBR increased by a factor of 3 ($p < 0.001$). Taking confirmed lesions only into account, we estimated a 10 % gain in additionally detected PSMA-positive lesions (7/70) within the patient cohort.

*Conclusions:* The time period between injection and data acquisition influences the detection rate of [$^{68}$Ga]PSMA-HBED-CC PET/CT. In biochemical recurrence with low PSA levels, late [$^{68}$Ga]PSMA-HBED-CC PET/CT imaging offers frequent advantages with regard to lesion contrast.

**Key words:** [$^{68}$Ga]PSMA-HBED-CC, PET, Early and late scans, Lesion detectability, PSMA

*Correspondence to:* M. Hohberg; *e-mail:* Melanie.Hohberg@uk-koeln.de

## Introduction

Early localization of biochemical recurrence (BCR) is challenging in clinical management of prostate cancer (PCa) after prostatectomy, radiotherapy, or any other local treatment [1]. If a prostate-specific membrane antigen (PSMA)-positive loco-regional tumor is detectable in patients with BCR, salvage lymphadenectomy or salvage radiotherapy offers the chance of long-term remission and postponement or avoidance of androgen deprivation therapy (ADT). In this context, the PSMA labeled with Ga-68 as a PET tracer has recently received increased attention in molecular imaging [2–6].

At many centers, [68Ga]PSMA-HBED-CC positron emission tomography (PET)/x-ray computed tomography (CT) imaging is routinely conducted 1 h (early) after tracer injection [7–9], but our understanding of pharmacodynamics in humans is limited. To study the impact of late imaging (3 h post-injection (p.i.)) using Ga-68-labeled PSMA, Rahbar et al. [10] analyzed 73 lesions in 20 patients and concluded that a late acquisition provided no additional benefit. In contrast, both Afshar-Oromieh et al. and Derlin et al. evaluated 112 and 88 patients respectively and found a higher tumor-to-background ratio [TBR] for most lesions in the case of late imaging [11, 12]. This observation was also confirmed by Schmuck et al. [13], who recorded a limited benefit in clinical routine for late imaging. Imaging at a late stage is feasible using F-18-labeled PSMA radiotracers owing to the longer half-life of F-18 in comparison with Ga-68 [14–16].

However, the reported advantage of a better tumor-to-background contrast in the late scans may be affected by the lower statistic count rate of late [68Ga]PSMA-HBED-CC PET/CT imaging. In order to improve the detection rate of [68Ga]PSMA-HBED-CC PET/CT, especially in the lower prostate-specific antigen (PSA) range compared with a one-time PET/CT acquisition protocol [16], we added late imaging to our routine data acquisition protocol. While other studies have described unclear findings in selected cases [11] or have included patients with high PSA levels (mean 20.6 µg/l, range 0.1 to 246 µg/l [12], mean 12.9 µg/l, range 0.02 to 700 µg/l [13]), we focused on patients with PSA levels < 2.0 µg/l. Our analysis aimed to investigate the detection rate of early, late, and dual-point PET/CT acquisition both qualitatively and quantitatively.

## Materials and Methods

### *Study Population*

Between June 2016 and February 2017, we used [68Ga]PSMA-HBED-CC PET/CT to examine 70 consecutive patients who had undergone prostatectomy and/or external beam radiation therapy for PCa and suffered BCR, but whose PSA levels were < 2.0 µg/l. The subgroup of patients who had not undergone prostatectomy but had undergone radiotherapy or had no local intervention received androgen deprivation therapy (ADT). In this subgroup, the PSA level measured was less than 2.0 µg/l during systemic treatment. All patients were subjected to [68Ga]PSMA-HBED-CC PET/CT.

This analysis was conducted in accordance with the Institutional Review Board (IRB). All patients gave written informed consent to PET imaging and inclusion of their data in a retrospective analysis. All procedures were performed in compliance with the regulations of the local authorities responsible (District Administration of Cologne, Germany).

### *Radiotracer*

[68Ga]PSMA-HBED-CC was synthesized by a fully automated, good-manufacturing-practice procedure, as previously described [16]. Ga-68 was obtained from a Ge-68/Ga-68 generator (ITM Isotopen Technologien München AG, Garching, Germany). The radiolabeling and purification of the PSMA ligand was performed with an automated radiosynthesizer. Radiochemical yield > 98 % was determined by systematic validation. The [68Ga]PSMA-HBED-CC solution was applied to the patient *via* an intravenous injection (mean 180 MBq, SD 43 MBq, median 176 MBq). Variation of injected radiotracer activity was caused by variable elution efficiencies during the lifetime of the Ge-68/Ga-68 generator.

### *PET/CT Acquisition and Image Reconstruction*

All PET/CT scans were performed on a Siemens Biograph mCT (mCT 128 Flow Edge, Siemens, Knoxville, USA). Early imaging started with a low-dose non-enhanced CT (120 kV, mA modulation, pitch 1.2, slice thickness 5.0 mm) for attenuation correction, followed by a whole body PET scan from the base of skull to mid-thigh at 1 h p.i. (mean 70 min, SD 15 min). Late imaging was performed 3 h after injection (mean 181 min, SD 13 min) of the lower abdomen and pelvis in all patients. Additionally, late imaging was performed by the physician's directive in one patient from another region. All emission data were corrected for attenuation, randoms, scatter, and decay. Reconstruction was conducted with an ordered subset expectation maximization (OSEM) algorithm with 4 iterations and 12 subsets and Gauss-filtered to a transaxial resolution of 5 mm at full-width at half-maximum (FWHM). The scan time was adjusted to get the same statistics in each scan.

### *Image Evaluation*

In addition to the clinical PET/CT report, all data sets were read independently on a syngo.via workstation (syngo.via VB20A Software, Siemens, Erlangen, Germany) by two experienced specialists for nuclear medicine (with 20 years'

experience in PET scan reading, certificate for CT reading) and any disagreements were resolved by consensus. The fused axial, coronal, and sagittal slices and the maximum intensity projection (MIP) were read visually. Suspicion of loco-regional relapse or metastases was based on functional imaging (*e.g.*, the intensity of the PSMA uptake) and on morphological criteria (*e.g.*, localization of lymph nodes, short-axis of lymph nodes, detection of osteolytic or osteoblastic lesions on the CT scan). The disparities in interpretation between the early and the late images resulted from a change in the visual contrast between the PSMA-positive lesion and the surrounding tissue/blood pool within the pelvic or abdominal scans. As the late PET/CT scans were restricted to the pelvis and the lower abdomen, we could not compare the late PSMA uptake in the lesions with the physiological uptake in the mediastinum, liver, or the parotid. A maximum of five lesions per patient with an appearance suggestive of PCa tissue were counted and analyzed. If metastases were found in more than one organ, we chose at least one representative lesion for each of the involved organs. Spherical volumes of interest were manually drawn around areas with focally increased uptake. Quantitative assessment of the uptake in lesions was performed by analysis of maximum (max) and peak SUV values. $SUV_{max}$ is defined as the hottest voxel within a volume of interest (VOI). $SUV_{peak}$ computes the mean SUV within a 1-$cm^3$ sphere positioned within a VOI so as to maximize that mean. In doing so, voxel super-sampling is performed where the dimensions are halved until they are less than or equal to 0.5 mm on each axis. Tumor-to-background ratio (TBR) and contrast-to-noise ratio (CNR) were calculated based on the following equations [17]:

$$\mathrm{TBR} = \frac{\mathrm{SUV_{max}(lesion)}}{\mathrm{SUV_{mean}(reference)}} \quad (1)$$

$$\mathrm{CNR} = \frac{\mathrm{SUV_{mean}(lesion)} - \mathrm{SUV_{mean}(reference)}}{\mathrm{SD(reference)}} \quad (2)$$

$SUV_{mean}$ and the corresponding standard deviation (SD) were measured in the gluteus muscle as reference region. Visual assessment was performed in terms of image quality and the presence or absence of halo artifacts and the residual activity within the ureters.

### *Validation of PET/CT Findings*

Many patients were referred by external urologists with different therapeutic concepts, which restricted the availability of follow-up data for validation of the PSMA-positive lesions. The following were taken as affirmative verification of lesions: positive histology of the PSMA-positive tissue within the prostate fossa, of the prostate gland, or of the removed lymph nodes from salvage lymphadenectomy; a decrease of the PSA level after salvage radiotherapy of the prostate fossa or of the PSMA-positive lymph nodes; a PSA decrease after radiotherapy of bone metastases, corresponding metastases on CT imaging, and the confirmation by imaging in the follow-up, respectively. When ADT was started after the [$^{68}$Ga]PSMA-HBED-CC PET/CT, the validation was indeterminate. Conflicting results between a PSMA-positive interpretation and a negative histology or a non-confirmative follow-up scan were reported separately.

### *Statistical Analysis*

Excel 2010 (Microsoft, Redmond, USA) and SPSS Statistics 22 (IBM, Armonk, USA) were used for statistical analysis and SUV values ($SUV_{max}$, $SUV_{peak}$) in the lesions, and their TBRs were compared between early and late acquisition using a Wilcoxon matched-pair signed-rank test. The Kolmogorov-Smirnov test and the Shapiro-Wilk test were used for testing for normality of the distributions. A $p$ value of $< 0.05$ was considered statistically significant.

## Results

### *Patient Characteristics*

The patients were on average 69 years old (range 49–83 years), with an average weight of 80 kg (range 68–120 kg). The average PSA value was 0.8 µg/l (range 0.6–2.0 µg/l). Sixty-four (91 %) patients had undergone radical prostatectomy with or without salvage radiotherapy, and 4 (6 %) patients had external beam radiation therapy (EBRT) as first-line treatment while 2 (3 %) patients were started on ADT without any local intervention. Twelve (17 %) patients had received ADT within the last 6 months prior to the examination. All patients with EBRT as first-line therapy were included in the patient subgroup with ADT. Details of the study population are summarized in Table 1.

### *Visual Analysis*

Of the 70 patients studied, 44 were interpreted as PSMA-positive while 26 patients were classified as loco-regional PSMA-negative within the PET fields, which were examined twice. A constellation of PSMA positivity outside the pelvis or the lower abdomen despite classification as PSMA-negative in the pelvis or the lower abdomen occurred in four cases. In the 44 PSMA-positive patients, we analyzed 70 suspicious PSMA-positive lesions, which included 21 bone lesions, 40 lymph nodes, and 9 local lesions within the prostate fossa.

Fifty-seven of the 70 lesions (79 %) were detected in both scans with a visibly equal PSMA intensity. Figure 1 shows the results from one patient in whom a suspicious lesion was detectable in both PET/CT scans. Ten lesions from seven

**Table 1.** Patient characteristics of the 70 consecutive patients. ADT, androgen deprivation therapy; SD, standard deviation; PSA, prostate-specific antigen

| Parameter | Value |
|---|---|
| Age [y] | |
| Mean ± SD | 68.9 ± 7.4 |
| Range | 49–83 |
| Activity [MBq] | |
| Mean ± SD | 180.2 ± 38.7 |
| Range | 120–281 |
| Gleason score | |
| Mean ± SD | 7.5 ± 1.0 |
| Range | 5–10 |
| PSA [µg/L] | |
| Mean ± SD | 0.8 ± 0.5 |
| Range | 0.4–1.9 |
| ADT | |
| Present | 12 |
| Absent | 58 |
| Early PET [min] | |
| Mean ± SD | 70 ± 15 |
| Range | 47–85 |
| Late PET [min] | |
| Mean ± SD | 181 ± 13 |
| Range | 153–194 |

different patients were detected in the scans 3 h p.i. but were not clearly identified at 1 h after injection. Without the addition of the late PET acquisition, five PET scans were originally read as completely PSMA-negative, and from the late positive PET interpretation, a local therapeutic consequence was drawn in five of the seven patients. On the other hand, three lesions from three different patients were easier to detect in the scan 1 h p.i. Examples are shown in Figs. 2 and 3.

Halo artifacts were observed in the 3-h p.i. measurements only, and occurred in 17/70 (24 %) patients. The presence of halo artifacts was not judged to lower the detectability of lesions. Residual activity within the ureters was present in 12/70 (17 %) patients in the early measurements and in 10/70 (14 %) patients in the late measurements but this also had no effect on detectability of lesions.

## *Quantitative Analysis*

Quantifying the late scans, 57/70 (81 %) of the suspicious lesions presented higher (mean + 32 %) $SUV_{max}$ values and 53/70 (76 %) higher (mean + 24 %) $SUV_{peak}$ values compared to $SUV_{max}$ and $SUV_{peak}$ values of the early scans. Additionally, 64/70 (91 %) of the suspicious lesions presented a higher (mean + 110 %) TBR and 56/70 (80 %) a higher (mean + 84 %) CNR at 3 h p.i. compared to 1 h after injection, as shown in Figs. 4 and 5. Statistical analysis showed all the differences in the $SUV_{max}$, $SUV_{peak}$, TBR, and CNR to be statistically significant ($p < 0.001$). None of the measured values were normally distributed, as assessed by the Kolmogorov-Smirnov test and the Shapiro-Wilk test (both $p < 0.05$). The mean SUV in the reference region decreased significantly over time (mean − 37 %, $p < 0.001$). These results are summarized in Tables 2 and 3.

Analyzing the suspicious PSMA-positive lesions with respect to their localization within lymph nodes, bones, or prostate fossa, similar results were found for the $SUV_{max}$ ($p < 0.001$) and $SUV_{peak}$ ($p < 0.001$) values and the CNRs ($p < 0.001$) for the three different types of lesions. The TBR was slightly but not significantly higher for local PSMA-positive tissue within the prostate fossa ($p = 0.008$) as compared to lymph nodes ($p < 0.001$) or bone lesions ($p < 0.001$).

## *Histopathological Findings and Follow-up Data*

From the 44 patients with PSMA-positive lesions, we were able to obtain clinical follow-up information in 33 cases. We

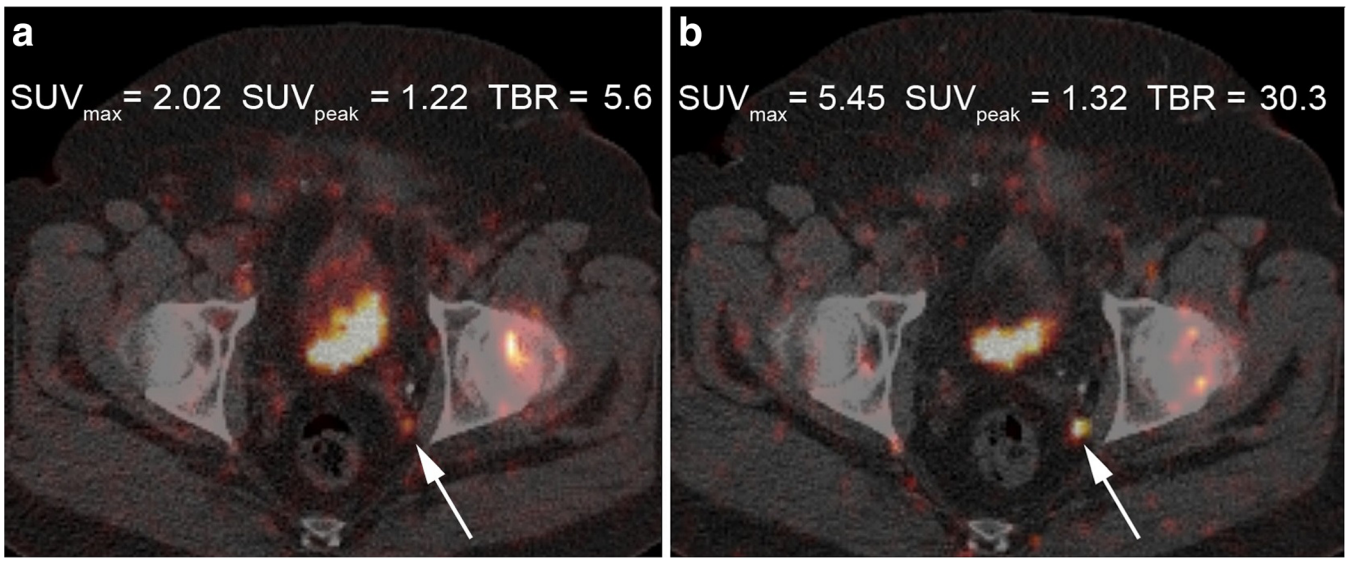


**Fig. 1.** [$^{68}$Ga]Ga-PSMA-HBED-CC PET/CT scans obtained at **a** 1 h and **b** 3 h p.i. One suspicious lesion (marked lymph node by an arrow) presented a higher uptake value for $SUV_{max}$, $SUV_{peak}$, and a higher TBR at 3 h p.i. compared to 1 h p.i. The scans were taken from patient no. 3 in Table 4.

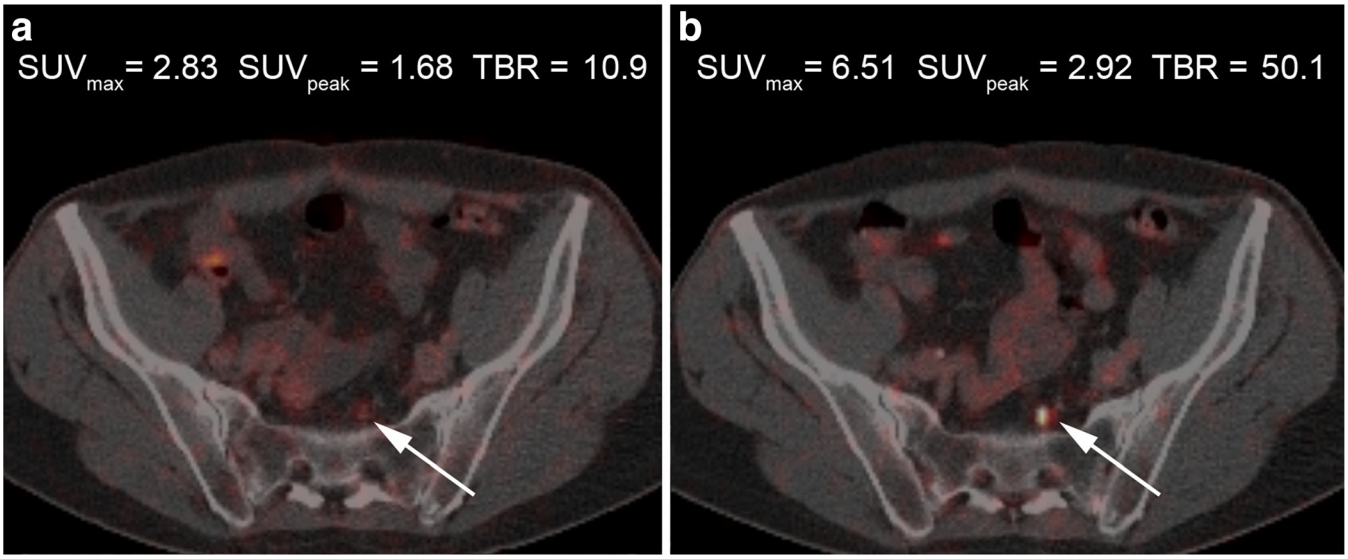


**Fig. 2.** [68Ga]Ga-PSMA-HBED-CC PET/CT scans obtained **a** 1 h and **b** 3 h p.i. One suspicious lesion (marked lymph node by an arrow) was visible only in the late images. The scans were taken from patient no. 1 in Table 4.

obtained confirmation of the PSMA-positive lesions in 26 patients, the interpretation remained indeterminate in 1 patient (who started with ADT), and conflicting results were obtained in 6 patients. The affirmative data for PSMA-positive tissue within the prostate fossa was based on biopsy and histology ($n = 2$), or on a decrease in the PSA level after salvage radiotherapy ($n = 2$). The affirmative data for PSMA-positive lymph nodes came from histology ($n = 4$), or a decrease in the PSA level after radiotherapy ($n = 6$), or a decrease in the PSA level after salvage lymphadenectomy, but histologic confirmation was lacking ($n = 1$). The PSMA-positive skeletal metastases were reflected in corresponding CT information ($n = 8$), or progressive disease, demonstrated by PSMA PET/CT scans on follow-up ($n = 2$), or a decrease in the PSA level after radiotherapy ($n = 1$). Conflicting results arose from negative biopsy of the prostate fossa in one patient, from negative histology of the removed lymph nodes with the decision to start with ADT in two patients, and from follow-up imaging without any intervention in three patients. The conflicting data for these six patients may potentially be attributed to false-positive PSMA-positive tissue, but do not provide unequivocal evidence of false-positive findings.

With regard to the ten patients with discordant PSMA-positive lesions in the early and late scans, nine without ADT and one with ADT, we have information on local interventions in seven cases (Table 4): Positive histology of lymph nodes metastases was found in patient no. 3. PSA levels were decreasing after radiotherapy of PSMA-positive lymph nodes in patient nos. 2 and 8. PSA level was

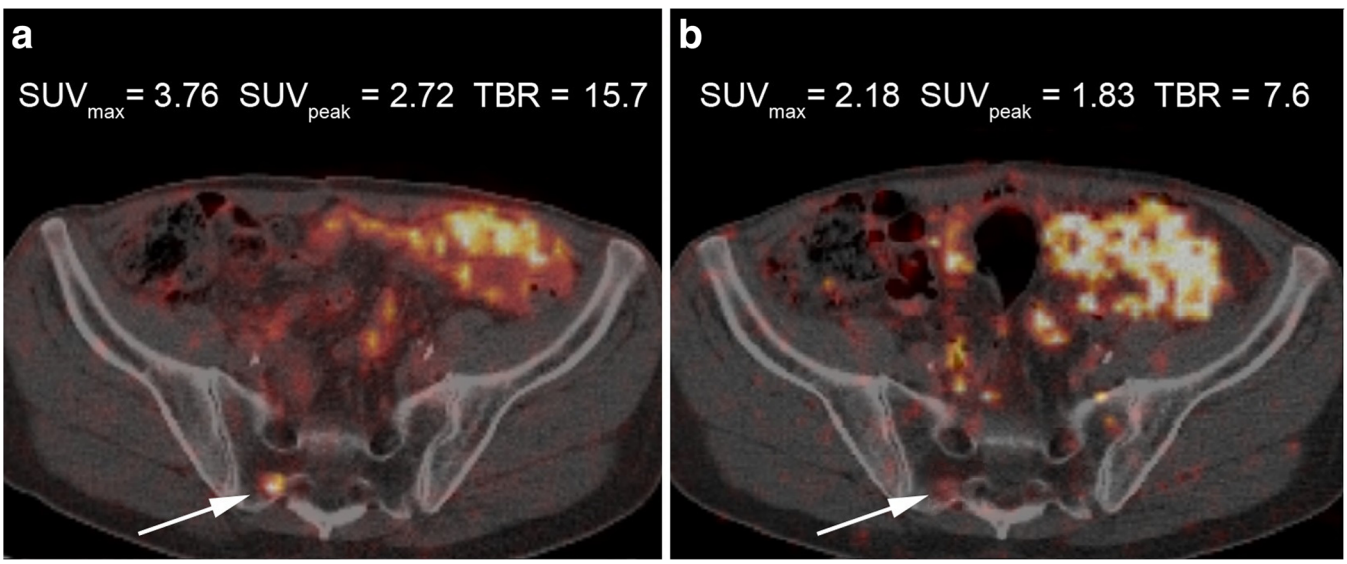


**Fig. 3.** [68Ga]Ga-PSMA-HBED-CC PET/CT scans obtained **a** 1 h and **b** 3 h p.i. One suspicious lesion (marked bone lesion by an arrow) was visible only in the early images. The scans were taken from patient no. 9 in Table 4.

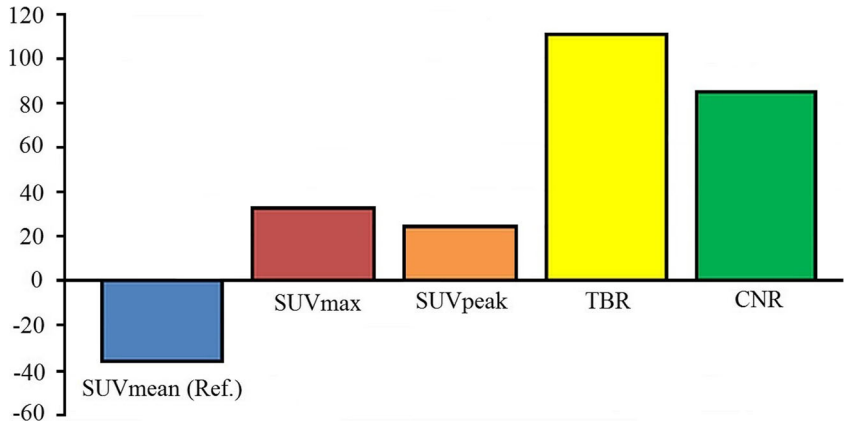


**Fig. 4.** Difference for mean SUVmax, SUVpeak, TBR, and CNR between 3 h p.i. and 1 h p.i.

decreasing after salvage lymphadenectomy in patient no. 1, but histologic confirmation is missing. In the follow-up of patient nos. 4 and 9 bone metastases were found PSMA-positive. Patient no. 5 was subjected to surgery after repeated salvage lymphadenectomy. Nodal metastases were histologically confirmed in each of the previous lymphadenectomies, but were not found by this third surgical intervention. ADT was then started without an additional PET scan. Three patients (patient nos. 6, 7, and 10) were not subjected to local interventions: The next follow-up PMSA PET/CT scan was completely negative in two of these three patients. Thus, a false-positive interpretation was probable regarding late PSMA-positive tissue in patient no. 7 and early PSMA-positive tissue in patient no. 10, respectively. Starting with ADT, verification was not possible in patient no. 6.

## Discussion

From our analysis of 70 consecutive patients with biochemically relapsed prostate cancer who underwent early and late [$^{68}$Ga]PSMA-HBED-CC PET/CT, we have learned that (1) late imaging provides additional information with significantly increased SUV in the majority of the PSMA-positive lesions, but that (2) a small number of lesions were better detected by early imaging 1 h p.i.

Delayed [$^{68}$Ga]PSMA-HBED-CC PET/CT imaging at 3 h p.i. has previously been reported to offer additional information to that acquired through imaging after 1 h in some selected patients [11, 18]. The intriguing idea of improving the detection of faint PSMA-positive lesions by a variation of timing was applied in our clinical routine setting in a consecutive sequence of patients.

Higher detection rates compared to ours were found by Hope et al. using [$^{68}$Ga]PSMA-HBED-CC [19] even for PSA values of less than 0.2 μg/l. One reason for these impressive results may be the use of higher applied activities and a longer emission scan in their study. The advantages of high activities of modified PSMA tracers might be an argument in favor of F-18-labeled PSMA tracers in the future [16, 20, 21].

We started with the patients referred due to biochemical recurrence or therapy monitoring and a relatively low PSA level of less than 2 μg/l. In this patient group with low PSA levels, disparity between early and late images with regard to a PSMA-positive lesion was found in 14 % of the cases. Even when taking a conservative approach and counting validated lesions only, additional PSMA-positive lesions were observed in 10 % of the patient cohort. In the case of

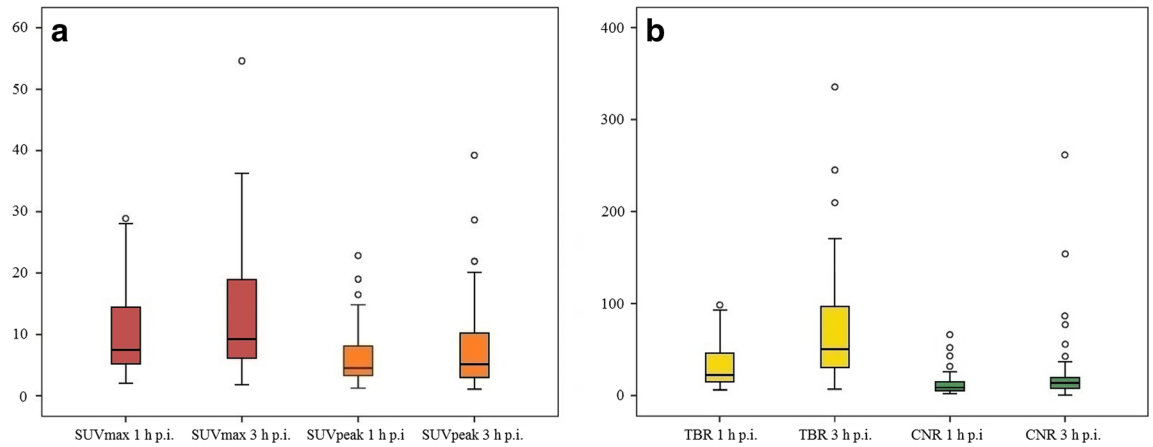


**Fig. 5.** Comparison of the values for **a** $SUV_{max}$ and $SUV_{peak}$, and **b** TBR and CNR obtained at 3 h p.i. and 1 h p.i. Whisker range within 1.5 IQR.

**Table 2.** Mean SUV values (tumor and reference region), tumor-to-background (TBR), and contrast-to-noise ratios (CNR) at 1 h and 3 h p.i. and corresponding *p* values for the 70 PSMA-positive lesions in 44 PSMA-positive patients

| | $SUV_{mean}$(Ref.) | $SUV_{peak}$ | $SUV_{max}$ | TBR | CNR |
|---|---|---|---|---|---|
| 1 h p.i. | 0.347 | 6.175 | 10.136 | 32.323 | 11.786 |
| 3 h p.i. | 0.220 | 7.658 | 13.366 | 67.934 | 36.470 |
| 3 h *vs.* 1 h p.i. | − 37 % ($p < 0.001$) | 24 % ($p < 0.001$) | 32 % ($p < 0.001$) | 110 % ($p < 0.001$) | 84 % ($p < 0.001$) |

discordant PSMA-positive lesions, late imaging offered advantages more often than early imaging. This may be explained by a higher internalization rate of the PSMA ligand in the late scans.

Of all the patients with PSMA-positive lesions, follow-up data was evaluable in 75 % and confirmation in 60 % of cases. In ten patients, discordant PSMA-positive lesions were reported in the early and late scans. Verification confirmed PSMA-positive lesions in seven out of these ten patients in accordance with the results of the late PET scan. False-positive lesions were assumed retrospectively in two patients. Verification was not possible in one patient. Our follow-up data were obtained from different referring urologists.

When therapeutic consequences such as salvage lymphadenectomy or salvage radiotherapy of the prostate fossa or salvage radiotherapy of the lymph nodes or radiotherapy of a singular bone metastasis were drawn, our interpretation, whether the PSMA PET/CT interpretation was true-positive or false-positive, remained difficult in some patients. The casuistically observed discrepancy between PSA decreases after salvage lymphadenectomy without histological confirmation highlighted the technical difficulty of finding such small PSMA-positive lesions intraoperatively or histologically. Small tumor tissue may be difficult to detect intraoperatively and may potentially be missed even on histopathological evaluation. Finally, the value of more sensitive tumor detection by means of PET imaging with regard to individual benefit in terms of improved progression free or overall survival is very difficult to assess.

There are some other possible strategies for technical improvement of PSMA PET/CT: early [$^{68}$Ga]PSMA-HBED-CC PET/CT imaging starting 5 min p.i. when the bladder is free from activity excreted with the urine [22] may provide more accurate information concerning local recurrence.

Our study question on the impact of early and late [$^{68}$Ga]PSMA-HBED-CC PET/CT scans was confined to biochemical recurrence or therapeutic monitoring based on a PSA level < 2 µg/l. It is probable that combined early and late PET scanning will delineate more PSMA-positive lesions in prostate cancer patients with PSA levels > 2 µg/l as well.

**Table 3.** Results of Wilcoxon test for 70 PSMA-positive lesions, detected in the bone ($n = 21$), in lymph nodes ($n = 40$), and in the prostatic fossa ($n = 9$). SUV, standardized uptake value; TBR, tumor-to-background ratio (TBR); CNR, contrast-to-noise ratio

| | | All lesions | Lymph nodes | Bone lesions | Local tissue |
|---|---|---|---|---|---|
| SUVmax 3 h p.i.—SUVmax 1 h p.i. | Negative ranks[a)] | 13 (18.6 %) | 9 (22.5 %) | 3 (14.2 %) | 2 (22.2 %) |
| | Positive ranks[b)] | 57 (81.4 %) | 31(77.5 %) | 18 (85.7 %) | 7 (77.8 %) |
| | Total | 70 (100 %) | 40 (100 %) | 21(100 %) | 9 (100 %) |
| | Z score | 5.713 | 4.207 | 3.354 | 2.073 |
| | *p* value | < 0.001 | < 0.001 | 0.001 | 0.038 |
| SUVpeak 3 h p.i.—SUVpeak 1 h p.i. | Negative ranks[c)] | 17 (24.3 %) | 9 (22.5 %) | 5 (23.8 %) | 3 (33.3 %) |
| | Positive ranks[d)] | 53 (75.7 %) | 31 (77.5 %) | 16 (76.2 %) | 6 (66.7 %) |
| | Total | 70 (100 %) | 40 (100 %) | 21(100 %) | 9 (100 %) |
| | Z score | 4.598 | 3.468 | 2.624 | 1.897 |
| | *p* value | < 0.001 | 0.001 | 0.009 | 0.058 |
| TBR 3 h p.i.—TBR 1 h p.i. | Negative ranks[e)] | 6 (8.6 %) | 5 (12.5 %) | 2 (9.5 %) | 0 (0 %) |
| | Positive ranks[f)] | 64 (91.4 %) | 35 (87.5 %) | 19 (90.5 %) | 9 (100 %) |
| | Total | 70 (100 %) | 40 (100 %) | 21(100 %) | 9 (100 %) |
| | Z score | 6.899 | 5.067 | 3.841 | 2.666 |
| | *p* value | < 0.001 | < 0.001 | < 0.001 | 0.008 |
| CNR 3 h p.i.—CNR 1 h p.i. | Negative ranks[g)] | 14 (20.0 %) | 8 (20.0 %) | 5 (23.8 %) | 2 (22.2 %) |
| | Positive ranks[h)] | 56 (80.0 %) | 32 (80.0 %) | 16 (76.2 %) | 7 (77.8 %) |
| | Total | 70 (100 %) | 40 (100 %) | 21 (100 %) | 9 (100 %) |
| | Z score | 5.673 | 4.422 | 2.902 | 1.955 |
| | *p* value | < 0.001 | < 0.001 | 0.004 | 0.051 |

[a)] $SUV_{max}$ 3 h p.i. < $SUV_{max}$ 1 h p.i.
[b)] $SUV_{max}$ 3 h p.i. > $SUV_{max}$ 1 h p.i.
[c)] $SUV_{peak}$ 3 h p.i. < $SUV_{peak}$ 1 h p.i.
[d)] $SUV_{peak}$ 3 h p.i. > $SUV_{peak}$ 1 h p.i.
[e)] TBR 3 h p.i. < TBR 1 h p.i.
[f)] TBR 3 h p.i. > TBR 1 h p.i.
[g)] CNR 3 h p.i. < CNR 1 h p.i.
[h)] CNR 3 h p.i. > CNR 1 h p.i.

**Table 4.** Patient characteristics and pathological tracer uptake in [68Ga]PSMA-HBED-CC PET/CT 1 h and 3 h after injection. ADT, androgen deprivation therapy; BCR, biochemical recurrence; LAD, lymphadenectomy; LN, lymph node; n.a., not available; p.i., post-injection; RT, radiotherapy; S-LAD, salvage lymphadenectomy; (), numbers in brackets refer to lesions that were discernible but not clearly visible

| Patient no. | Age (years) | PSA (µg/L) | Indication Gleason | Activity (MBq) timing | local PSMA + | Nodal PSMA + | Distant PSMA + | Therapeutic consequence | Verification |
|---|---|---|---|---|---|---|---|---|---|
| 1 | 52 | 0.29 | BCR after prostatectomy 4 + 3 | 233<br>1 h<br>3 h | <br>0<br>0 | <br>0<br>1 left iliacal | <br>0<br>0 | S-LAD | Histologically not confirmed. PSA decrease to 0.11 ng/mL. After 4 months PET/CT PSMA-negative. |
| 2 | 66 | 0.6 | BCR after prostatectomy and S-LAD 3 + 4 | 202<br>1 h<br>3 h | <br>0<br>0 | <br>4<br>5 | <br>0<br>0 | RT of pelvic LN | PSA decrease to 0.3 ng/mL |
| 3 | 64 | 0.53 | BCR after prostatectomy 4 + 3 | 176<br>1 h<br>3 h | <br>0<br>0 | <br>2 pre-sacral<br>3 pre-sacral and paravesical | <br>0<br>0 | S-LAD | 4 LN metastases histologically confirmed |
| 4 | 65 | 0.27 | BCR after prostatectomy and S-LAD 5 + 5 | 229<br>1 h<br>3 h | <br>0<br>0 | <br>0<br>0 | <br>(4)<br>4 | RT Th 6 and docetaxel | CT osteosclerotic lesions |
| 5 | 72 | 1.3 | BCR after prostatectomy and S-LAD 3 + 4 | 161<br>1 h<br>3 h | <br>0<br>0 | <br>0<br>1 left iliacal | <br>0<br>0 | Second S-LAD (histologically confirmed LN metastasis in the S-LAD before and in the initial operation) | LN not found and histologically not confirmed, after 6 months PSA increase to 4.5, then ADT |
| 6 | 69 | 0.48 | BCR after prostatectomy 3 + 4 | 132<br>1 h<br>3 h | <br>(1)<br>1 | <br>0<br>0 | <br>0<br>0 | ADT | After 18 months treated with ADT PSA progression to 1.34 ng/mL |
| 7 | 66 | 0.98 | BCR after prostatectomy and S-LAD 3 + 4 | 191<br>1 h<br>3 h | <br>(1)<br>1* | <br>0<br>0 | <br>0<br>0 | Wait and see | 18F-PSMA PET/CT 9 months later: PSMA-positive pulmonary metastases. No tracer accumulation in the pelvis. |
| 8 | 66 | 0.7 | BCR after prostatectomy 4 + 3 | 172<br>1 h<br>3 h | <br>0<br>0 | <br>1<br>(1) | <br>0<br>0 | RT of LN area | PSA decrease to 0.5 ng/mL |
| 9 | 72 | 0.789 ADT | Therapy monitoring under ADT, previously prostatectomy and RT and ChT 4 + 5 | 110<br>1 h<br>3 h | <br>0<br>0 | <br>0<br>0 | <br>1 Os sacrum (1) | RT os sacrum | CT correlation. After 12 months, 3 new skeletal metastases and 3 PSMA-positive LN shown by 18F-PSMA PET/CT. PSA 9.5 without ADT |
| 10 | 70 | 0.22 | BCR after prostatectomy | 237<br>1 h<br>3 h | <br>0<br>0 | <br>1*<br>0 | <br>0<br>0 | Wait and see | After 14 months PSA 0.24, 18F-PSMA PET/CT negative |

*Probable false-positive tissue on the early or late [68Ga]PSMA-HBED-CC PET/CT scan

The results from this study have demonstrated that the timing of [68Ga]PSMA-HBED-CC PET/CT imaging has an influence on the detection rate of this imaging procedure. In general, late PET/CT scans were superior compared to early PET/CT scans in terms of detection and lesion visibility. Seventy-five percent of all analyzed parameters ($SUV_{max}$, $SUV_{peak}$, TBR, CNR) increased significantly over time. The highest possible detection rate was reached by the combination of early and late imaging of the pelvis and the abdomen.

However, as late [68Ga]PSMA-HBED-CC PET/CT scans were restricted to the region of the lower abdomen and pelvis, PSMA-positive lesions outside that region may have been missed. Performing early and late [68Ga]PSMA-HBED-CC PET/CT imaging requires a more extensive protocol for clinical routine. This is an important aspect for modern health care systems which continuously pushes the boundaries of efficacy. The key question is therefore whether a procedure can be found that provides the best possible information available by [68Ga]PSMA-HBED-CC PET/CT in a single session. Future studies should investigate whether or not imaging is optimal 2 h after injection, as optimal lesion detection was obtained for F-18-labeled PSMA [21] at that time point.

## Conclusion

In biochemical recurrence with low PSA levels, less than 2 µg/l late [68Ga]PSMA-HBED-CC PET/CT imaging 3 h

p.i. frequently improved the visibility of small PSMA-positive lesions compared to PET scans 1 h p.i. In view of the possible local therapeutic interventions, additional late PET scans in BCR (restricted to pelvis and lower abdomen) can be recommended, when the PSA level is low without ADT. However, it may be worthwhile continuing to take a scan at 1 h p.i., because [$^{68}$Ga]PSMA-HBED-CC PET/CT early and late imaging offered the best available information.

**Compliance with Ethical Standards.** This analysis was conducted in accordance with the Institutional Review Board (IRB). All patients gave written informed consent to PET imaging and inclusion of their data in a retrospective analysis. All procedures were performed in compliance with the regulations of the local authorities responsible (District Administration of Cologne, Germany).

### *Conflict of Interest*

The authors declare that they have no conflict of interest.

## References


1. Cornford P, Bellmunt J, Bolla M, Briers E, de Santis M, Gross T, Henry AM, Joniau S, Lam TB, Mason MD, van der Poel HG, van der Kwast TH, Rouvière O, Wiegel T, Mottet N (2017) EAU-ESTRO-SIOG guidelines on prostate cancer. Part II: treatment of relapsing, metastatic, and castration-resistant prostate cancer. Eur Urol 71:630–642
2. Hillier SM, Maresca KP, Femia FJ, Marquis JC, Foss CA, Nguyen N, Zimmerman CN, Barrett JA, Eckelman WC, Pomper MG, Joyal JL, Babich JW (2009) Preclinical evaluation of novel glutamate-urea-lysine analogues that target prostate-specific membrane antigen as molecular imaging pharmaceuticals for prostate cancer. Cancer Res 69:6932–6940
3. Eder M, Schäfer M, Bauder-Wüst U, Hull WE, Wängler C, Mier W, Haberkorn U, Eisenhut M (2012) Ga-68-complex lipophilicity and the targeting property of a urea-based PSMA inhibitor for PET imaging. Bioconjug Chem 23:688–697
4. Schäfer M, Bauder-Wüst U, Leotta K, Zoller F, Mier W, Haberkorn U, Eisenhut M, Eder M (2012) A dimerized urea-based inhibitor of the prostate-specific membrane antigen for Ga-68-PET imaging of prostate cancer. EJNMMI Res 2:23
5. Bander NH (2006) Technology insight: monoclonal antibody imaging of prostate cancer. Nat Clin Pract Urol 3:216–225
6. Liu H, Moy P, Kim S, Xia Y, Rajasekaran A, Navarro V, Knudsen B, Bander NH (1997) Monoclonal antibodies to the extracellular domain of prostate-specific membrane antigen also react with tumor vascular endothelium. Cancer Res 57:3629–3634
7. Eiber M, Maurer T, Souvatzoglou M, Beer AJ, Ruffani A, Haller B, Graner FP, Kubler H, Haberhorn U, Eisenhut M, Wester HJ, Gschwend JE, Schwaiger M (2015) Evaluation of hybrid [68Ga]PSMA ligand PET/CT in 248 patients with biochemical recurrence after radical prostatectomy. J Nucl Med 56:668–674
8. Rauscher S, Maurer T, Fendler WP et al (2016) [$^{68}$Ga]PSMA ligand PET/CT in patients with prostate cancer: how we review and report. Cancer Imaging 16:14
9. Sahlmann CO, Meller B, Bouter C, Ritter CO, Ströbel P, Lotz J, Trojan L, Meller J, Hijazi S (2016) Biphasic [$^{68}$Ga]PSMA-HBED-CC-PET/CT in patients with recurrent and high-risk prostate carcinoma. Eur J Nucl Med Mol Imaging 43:898–905
10. Rahbar K, Vehren T, Boegemann M et al (2015) Dual time point PET/CT acquisition using Ga-68-PSMA-Radioligand. J Nucl Med 56(supplement 3):1437
11. Afshar-Oromieh A, Sattler LP, Mier W, Hadaschik BA, Debus J, Holland-Letz T, Kopka K, Haberkorn U (2017) The clinical impact of additional late PET/CT imaging with [$^{68}$Ga]PSMA-11 (HBED-CC) in the diagnosis of prostate cancer. J Nucl Med 58:750–755
12. Derlin T, Weiberg D, von Klot C, Wester HJ, Henkenberens C, Ross TL, Christiansen H, Merseburger AS, Bengel FM (2016) [$^{68}$Ga]PSMA I&T PET/CT for assessment of prostate cancer: evaluation of image quality after forced diuresis and delayed imaging. Eur Radiol 26:4345–4353
13. Schmuck S, Nordlohne S, von Klot CA, Henkenberens C, Sohns JM, Christiansen H, Wester HJ, Ross TL, Bengel FM, Derlin T (2017) Comparison of standard and delayed imaging to improve the detection rate of [$^{68}$Ga]PSMA I&T PET/CT in patients with biochemical recurrence or prostate-specific antigen persistence after primary therapy for prostate cancer. Eur J Nucl Med Mol Imaging 44:960–968
14. Rowe SP, Macura KJ, Mena E, Blackford AL, Nadal R, Antonarakis ES, Eisenberger M, Carducci M, Fan H, Dannals RF, Chen Y, Mease RC, Szabo Z, Pomper MG, Cho SY (2016) PSMA-based [$^{18}$F]DCFPyL PET/CT is superior to conventional imaging for lesion detection in patients with metastatic prostate Cancer. Mol Imaging Biol 18:411–419
15. Wondergem M, van der Zant FM, Knol RJJ, Lazarenko SV, Pruim J, de Jong IJ (2017) $^{18}$F-DCFPyL PET/CT in the detection of prostate cancer at 60 and 120 minutes: detection rate, image quality, activity kinetics, and biodistribution. J Nucl Med 58:1797–1809
16. Dietlein F, Kobe C, Neubauer S, Schmidt M, Stockter S, Fischer T, Schomäcker K, Heidenreich A, Zlatopolskiy BD, Neumaier B, Drzezga A, Dietlein M (2017) PSA-stratified performance of F-18 and Ga-68-PSMA PET in patients with biochemical relapse of prostate cancer. J Nucl Med 58:947–952
17. Yan J, Schaefferkoetter J, Conti M, Townsend D (2016) A method to assess image quality for low-dose PET: analysis of SNR, CNR, bias and image noise. Cancer Imaging 16:26
18. Afshar-Oromieh A, Hetzheim H, Kübler K et al (2016) Radiation dosimetry of [$^{68}$Ga]PSMA-11 (HBED-CC) and preliminary evaluation of optimal imaging timing. Eur J Nucl Med Mol Imaging 43:1611–1620
19. Hope TA, Aggarwal R, Chee B et al (2018) Impact of [$^{68}$Ga]PSMA-11 PET on management in patients with biochemically recurrent prostate cancer. J Nucl Med 58:1956–1961
20. Dietlein M, Kobe C, Kuhnert G, Stockter S, Fischer T, Schomäcker K, Schmidt M, Dietlein F, Zlatopolskiy BD, Krapf P, Richarz R, Neubauer S, Drzezga A, Neumaier B (2015) Comparison of [$^{18}$F]DCFPyL and [$^{68}$Ga]Ga-PSMA-HBED-CC for PSMA-PET imaging in patients with relapsed prostate cancer. Mol Imaging Biol 17:575–584
21. Szabo Z, Mena E, Rowe SP, Plyku D, Nidal R, Eisenberger MA, Antonarakis ES, Fan H, Dannals RF, Chen Y, Mease RC, Vranesic M, Bhatnagar A, Sgouros G, Cho SY, Pomper MG (2015) Initial evaluation of [$^{18}$F]DCFPyL for prostate-specific membrane antigen (PSMA)-targeted PET imaging of prostate cancer. Mol Imaging Biol 17:565–574
22. Uprimny C, Kroiss AS, Fritz J, Decristoforo C, Kendler D, von Guggenberg E, Nilica B, Maffey-Steffan J, di Santo G, Bektic J, Horninger W, Virgolini IJ (2017) Early PET imaging with [68]Ga-PSMA-11 increases the detection rate of local recurrence in prostate cancer patients with biochemical recurrence. Eur J Nucl Med Mol Imaging 44:1647–1655